The physical state of water in bacterial spores

Erik P. Sunde[a], Peter Setlow[b], Lars Hederstedt[c], and Bertil Halle[a,1]

[a]Department of Biophysical Chemistry, Center for Molecular Protein Science, Lund University, SE-22100 Lund, Sweden; [b]Department of Molecular, Microbial, and Structural Biology, University of Connecticut Health Center, Farmington, CT 06030-3305; and [c]Department of Cell and Organism Biology, Lund University, SE-22362 Lund, Sweden

Edited by Richard M. Losick, Harvard University, Cambridge, MA, and approved September 23, 2009 (received for review July 31, 2009)

The bacterial spore, the hardiest known life form, can survive in a metabolically dormant state for many years and can withstand high temperatures, radiation, and toxic chemicals. The molecular basis of spore dormancy and resistance is not understood, but the physical state of water in the different spore compartments is thought to play a key role. To characterize this water in situ, we recorded the water ^{2}H and ^{17}O spin relaxation rates in D_2O-exchanged *Bacillus subtilis* spores over a wide frequency range. The data indicate high water mobility throughout the spore, comparable with binary protein–water systems at similar hydration levels. Even in the dense core, the average water rotational correlation time is only 50 ps. Spore dormancy therefore cannot be explained by glass-like quenching of molecular diffusion but may be linked to dehydration-induced conformational changes in key enzymes. The data demonstrate that most spore proteins are rotationally immobilized, which may contribute to heat resistance by preventing heat-denatured proteins from aggregating irreversibly. We also find that the water permeability of the inner membrane is at least 2 orders of magnitude lower than for model membranes, consistent with the reported high degree of lipid immobilization in this membrane and with its proposed role in spore resistance to chemicals that damage DNA. The quantitative results reported here on water mobility and transport provide important clues about the mechanism of spore dormancy and resistance, with relevance to food preservation, disease prevention, and astrobiology.

Bacillus subtilis | hydration | magnetic relaxation dispersion | spore dormancy | spore resistance

When deprived of nutrients, *Bacillus* and *Clostridium* bacteria form endospores that can survive in a metabolically dormant state for years yet can transform into vegetative cells within minutes, triggered by environmental signals. Bacterial spores not only survive starvation, but are also highly resistant to heat, radiation, and toxic chemicals (1, 2). Because of their exceptional ability to survive adverse conditions for long periods, bacterial spores are major causes of food spoilage and food-borne disease, and they might even serve as vehicles for transfer of life between planets (3). Furthermore, *Bacillus anthracis* spores pose a threat as a potential agent of biological warfare and terrorism. For these reasons, it is important to elucidate the molecular mechanisms of spore dormancy and resistance. This task is challenging because it involves several fundamental biophysical phenomena which are themselves not fully understood, including protein stability and mobility, membrane permeability, and control of enzymatic activity.

The thermal stability of native protein conformations is largely governed by solvent-mediated interactions (4), and enzymatic activity relies on conformational changes and molecular associations that are strongly coupled to solvent mobility. Both the heat resistance and the metabolic dormancy of spores may therefore be largely controlled by the physical state and chemical composition of the solvent. Anhydrobiotic organisms—including plant seeds, yeast cells, and certain plants and invertebrates—achieve dormancy by replacing most of the cell water by compatible osmolytes, such as trehalose or sucrose, thereby transforming the cytoplasm into a metastable glassy state (5, 6). Although bacterial spores do not accumulate glass-forming osmolytes, it has been proposed that the spore's core region is also in a glassy state (7–9). If so, spore dormancy could simply be attributed to the extreme retardation of diffusive molecular motions in the highly viscous glass state. Furthermore, heat resistance might then be explained in kinetic rather than thermodynamic, terms. An endothermic transition observed by differential scanning calorimetry on *Bacillus subtilis* spores was initially assigned to a glass transition (9), but this interpretation has been questioned (10). On the other hand, at least some core components appear to be immobilized. Dielectric permittivity data (11) and electron paramagnetic resonance spectra (12) suggest that most ions in the core are immobilized, ^{13}C NMR spectroscopy indicates that the core's large depot of pyridine-2,6-dicarboxylic acid (dipicolinic acid, DPA) is in a solid-like state (13), and fluorescence measurements show that green fluorescent protein is at least 4 orders of magnitude less mobile in the dormant core than in the cytoplasm of the vegetative *B. subtilis* cell (14). Although these observations are consistent with a glassy core, attempts using ^{1}H NMR linewidths to directly measure water mobility in spores have not been conclusive (15, 16), partly because of the confounding effect of paramagnetic Mn(II) ions.

Whether glass-like or not, the core, even in fully hydrated spores, has a remarkably low water content, which correlates with the spore's heat resistance (17). The core contains the genome, about half of the spore's proteins, and a high concentration of calcium and other divalent ions chelated by DPA (1, 2). The core is surrounded by the cortex, a highly hydrated, cross-linked peptidoglycan matrix (18) that is thought to maintain the dehydrated state of the core (Fig. 1). The spore's outermost protective barrier, known as the coat, is composed of multiple layers of cross-linked proteins (19, 20). The coat provides resistance to chemicals and protects the cortex from hydrolytic enzymes. The spore has two membranes. The outer membrane, located just inside the coat, may not retain its integrity in the mature spore and, in any case, it is not a significant permeability barrier (2). The inner membrane (IM) that envelops the core may exist partly in a gel state with largely immobile lipids (21). The low permeability of the IM to ionic species and even to small nonionic solutes like methylamine has been linked to its role in protecting the core DNA from chemical attack (2).

Nuclear magnetic relaxation is among the few techniques that can yield quantitative information about the physical state of water in complex biological systems, but the interpretation of the measured spin relaxation rates is rarely straightforward (22). To separate contributions from water motions on different time scales, it is necessary to measure the longitudinal spin relaxation rate R_1 over a wide range of resonance frequencies ν_0. By using an array of NMR instruments, including fast field-cycling magnets as well as conventional high-field magnets, a so-called magnetic relaxation dispersion (MRD) profile, $R_1(\nu_0)$, can be recorded that spans 5 orders of magnitude in frequency (10^3-10^8 Hz for ^{2}H). The MRD profile is

Author contributions: E.P.S., P.S., L.H., and B.H. designed research; E.P.S. performed research; P.S. and L.H. contributed new reagents/analytic tools; E.P.S. and B.H. analyzed data; and E.P.S. and B.H. wrote the paper.

The authors declare no conflict of interest.

This article is a PNAS Direct Submission.

[1]To whom correspondence should be addressed. E-mail: bertil.halle@bpc.lu.se.

This article contains supporting information online at www.pnas.org/cgi/content/full/0908712106/DCSupplemental.

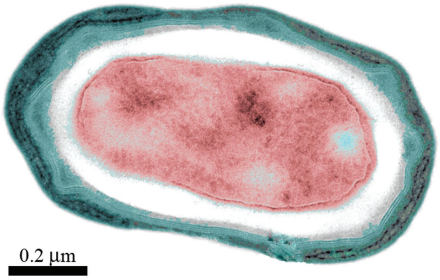

Fig. 1. Transmission electron micrograph of a wild-type (WT) *B. subtilis* endospore (60), with the principal regions color coded: core (red), cortex (white), and coat (green).

essentially a frequency mapping of the distribution of rotational correlation times for all water molecules in the sample. Recent ^{2}H MRD studies of living bacteria (23) have shown that cell water conforms to the expectations based on MRD studies of model systems (24). Here we use the same approach to characterize water dynamics in fully hydrated dormant spores of *B. subtilis*. In addition, we have measured the high-frequency relaxation rate of water ^{17}O spins. In general, the ^{2}H and ^{17}O nuclides are preferable to ^{1}H because they relax by a single-spin mechanism (involving the nuclear electric quadrupole) and hence provide direct information about the molecular rotational mobility (25), which is closely related to the (local) viscosity. In addition, the ^{2}H and ^{17}O relaxation rates are less affected than the ^{1}H rate by paramagnetic ions. Finally, the ^{17}O relaxation rate reports exclusively on water molecules, whereas the ^{1}H and (to a lesser extent) ^{2}H rates may contain a pH-dependent contribution from macromolecular OH and NH hydrogens that exchange with water hydrogens on the NMR relaxation time scale (22).

Because the key to dormancy and heat resistance is believed to reside in the core, the mobility of core water is of particular interest. H_2O/D_2O exchange studies demonstrate that external water exchanges with at least 96% of spore water (26), but our data show that water exchange across the IM is slow on the ^{2}H NMR relaxation time scale (20 ms). This allows us to separately assess water mobility inside and outside the core. We use the Mn(II)-induced ^{2}H spin relaxation to identify the magnetization component associated with the core, but we remove Mn(II) ions outside the core by EDTA to reveal the water dynamics in the cortex and coat. Further information was obtained by examining coat-deficient spores from a *B. subtilis* strain with mutations in the *cotE* and *gerE* genes (27). Unexpectedly, we found that the water permeability of the IM is greatly enhanced in these coat-deficient spores.

Results

Spatial Distribution and Hydration of Mn(II) Ions. Fig. 2 (black symbols) shows a water-^{2}H MRD profile spanning five frequency decades, measured on a sample of packed, fully hydrated WT *B. subtilis* spores. The MRD profile has two prominent features: a large-amplitude dispersion below ≈1 MHz and a broad maximum near 6 MHz. As discussed below (*Internal Water in Coat Proteins*), the low-frequency dispersion is produced by 0.14% of the spore water, transiently trapped in protein cavities. The MRD maximum is the hallmark of a paramagnetic relaxation enhancement (PRE) induced by the magnetic dipole–dipole coupling between unpaired electron spins of slowly tumbling paramagnetic ions, such as protein-bound Mn(II), and ^{2}H (or ^{1}H) spins in directly coordinated water molecules (28, 29). Manganese is present in our spore preparation at a high level of 84 μmol (g dry mass)$^{-1}$ (Table S1 of the *SI Appendix*). Other paramagnetic ions are much less abundant (Table S1 of the *SI Appendix*) and produce (at a given concentration) a much smaller PRE than Mn(II) (29).

The observed ^{2}H relaxation rate is the sum of a quadrupolar

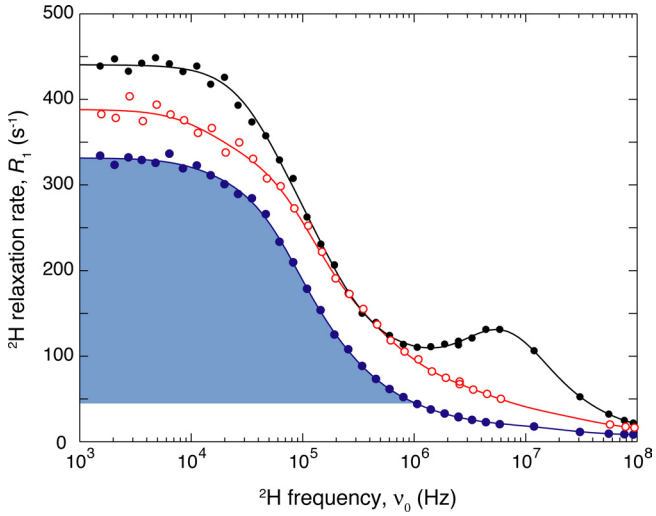

Fig. 2. Water-^{2}H MRD profiles from *B. subtilis* spores at 27° C and pH 7.6: untreated WT (black), EDTA-treated WT (blue), and EDTA-treated mutant (red). All R_1 data refer to a water content of 1.20 g D_2O (g dry mass)$^{-1}$. The curves are multi-Lorentzian numerical representations used for the model-free analysis. The blue-colored area is the contribution from internal water molecules with residence time >160 ns. The difference between the upper (black) and lower (blue) curves represents the PRE produced by Mn(II) ions outside the core.

contribution, which contains the desired information about spore-water rotational dynamics (22), and a PRE contribution. To eliminate the Mn(II)-induced PRE contribution, we treated the spores with the chelating agent EDTA. The MRD profile for EDTA-treated spores (Fig. 2, blue symbols) lacks the characteristic PRE maximum, and it can be represented with a sum of Lorentzian spectral densities, as for diamagnetic samples of immobilized proteins (23, 24).

Elemental analysis showed that EDTA treatment removes only 32% of spore manganese (Table S1 of the *SI Appendix*). Because the MRD profile from EDTA-treated spores does not have a PRE contribution (Fig. 2), we conclude that 68% of the Mn(II) ions in the spore are "invisible" to water ^{2}H relaxation. Two well-established facts strongly suggest that these invisible and nonextractable Mn(II) ions are located in the core. First, microanalytical studies identify the core as the major locus of mineral ions, with lesser amounts present in the coat (1). Second, the IM is essentially impermeable to ionic species (2). Neither Mn(II) ions nor EDTA are therefore expected to cross the IM on the 4-h time scale of the EDTA treatment. For the same reason, EDTA treatment removed only 10% of the large Ca^{2+} content of the spore (Table S1 of the *SI Appendix*).

The PRE contribution, obtained from the difference of the black and blue MRD data in Fig. 2, was analyzed quantitatively with the aid of the conventional Solomon–Bloembergen–Morgan theory (29, 30). A satisfactory agreement was obtained with parameter values in the expected ranges (see Text and Fig. S1 in the *SI Appendix*). In particular, the analysis indicates that the "visible" Mn(II) ions, located outside the core, have one water ligand on average.

Decomposition of the ^{2}H Relaxation Rate. The water-^{2}H magnetization relaxes biexponentially in both untreated and EDTA-treated spores (Fig. 3), implying slow water exchange between two compartments (31). Biexponential fits to the ^{2}H magnetization recovery at 92.1 MHz yield local relaxation rates for the two regions and the water fraction in each region (Table 1). The water distribution is the same for untreated and EDTA-treated spores, with 12% of sample water in the minor fraction and 88%

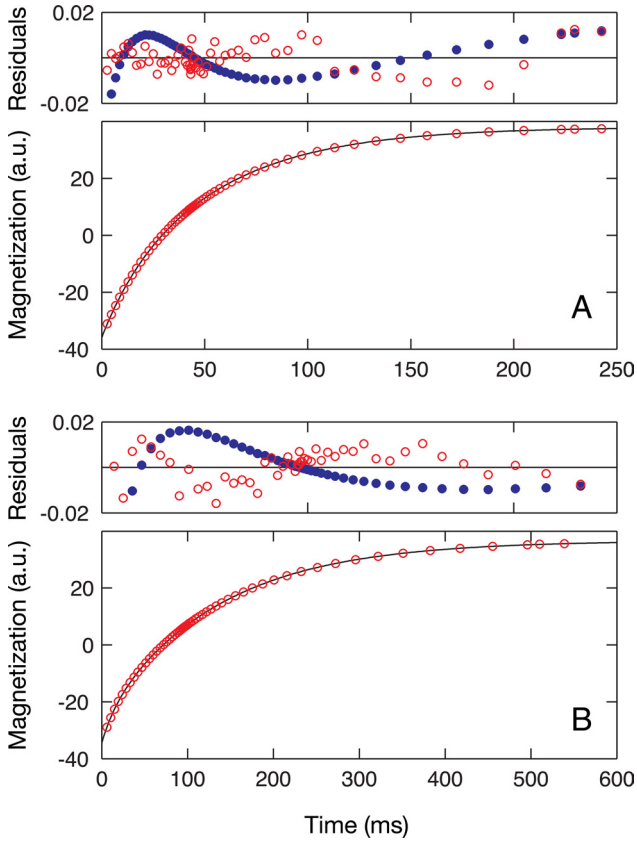

Fig. 3. Water-^{2}H magnetization recoveries at 92.1 MHz from untreated (*A*) and EDTA-treated (*B*) WT *B. subtilis* spores. The lower frames show experimental data and biexponential fits with parameter values as given in Table 1. The upper frames show the residuals for monoexponential (solid blue circles) and biexponential (open red circles) fits, with the former divided by a factor 50 to fit on the same scale.

in the major fraction. Because the IM is the only strong permeability barrier in the spore (2), we associate these water fractions with the core (cr) and noncore (ncr) regions of the sample. The ncr region comprises the cortex (cx), the coat (ct), and the external (ex) interstitial volume in the spore pellet (Fig. 1). Furthermore, we assign the minor fraction to the core region for the following reasons. First, 12% is in the range expected for the core-water fraction of *B. subtilis* spores (17, 32). Second, the minor fraction has the largest relaxation rate (Table 1), as expected from the lower water content of the core (17, 32). Third, because EDTA removes Mn(II) ions from the ncr region but not from the core (see *Spatial Distribution and Hydration of Mn(II) Ions*), EDTA-treatment should reduce the ^{2}H relaxation rate for the major (ncr) fraction but should not affect the rate for the minor (core) fraction. As seen from Table 1, this is indeed the case.

Spatially Resolved Spore Water Dynamics. The biexponential ^{2}H relaxation caused by slow water exchange across the IM makes

Table 1. Results of fits to water-^{2}H magnetization recovery at 92.1 MHz

Sample	f_{cr}	R_1^{cr} (s^{-1})	R_1^{ncr} (s^{-1})
WT	0.121 (4)	68.6 (3)	19.40 (1)
WT + EDTA	0.116 (4)	67.1 (5)	7.56 (1)
Mutant + EDTA	–	16.33 (1)	

Errors (one standard deviation) in the last digit are given in parentheses.

Table 2. Water fraction and dynamic perturbation factor for different spore regions

Strain	Region	f_k*	ξ_k†
WT	cr	0.12 (1)	30.8 (5)
WT	ncr	0.88 (1)	3.48 (1)
WT	cx + ct	0.58 (5)	4.8 (4)
cotE gerE mutant	cr + ncr	1	7.51 (1)

Errors (one standard deviation) in the last digit are given in parentheses. cr, core; cx, cortex; ct, coat; ex, external interstitial space; ncr, cx + ct + ex.
*Fraction of sample water in region *k*.
†Dynamic perturbation factor for region *k*.

it possible to separately assess water mobility in the different spore compartments. We quantify water mobility in region k by the dynamic perturbation factor (DPF), $\xi_k \equiv \langle\tau_R^k\rangle/\tau_R^0$, that is, the rotational correlation time averaged over all water molecules in region k divided by the same quantity in bulk water. To an excellent approximation (23), the DPF can be obtained in a model-independent way as the ratio of the high-frequency ^{2}H relaxation rate in region k, $R_1^k(\nu_0^*)$, and the (frequency-independent) relaxation rate in bulk water, R_1^0, that is $\xi_k = R_1^k(\nu_0^*)/R_1^0$. By using the highest experimental frequency, $\nu_0^* =$ 92.1 MHz, we include in the average $\langle\tau_R^k\rangle$ all water molecules with correlation times shorter than $1/(2\pi\nu_0^*) \approx 2$ ns (23). The DPF thus includes essentially all water molecules in the hydration layers of proteins and other solutes (33), but not internal water molecules buried in small polar cavities inside proteins or at the interfaces of tightly associated macromolecules.

By using the local relaxation rates $R_1^k(\nu_0^*)$ in Table 1 and $R_1^0 =$ 2.175 s^{-1} (measured for bulk D_2O at 27° C), we can calculate the DPF for the core and ncr regions (Table 2). For core water, we thus obtain $\xi_{cr} = 30.8 \pm 0.5$. The ncr region includes the ex volume in the spore pellet. This volume is essentially bulk water, so $\xi_{ex} = 1$. Subtracting this trivial contribution from ξ_{ncr}, we find $\xi_{cx+ct} = 4.8 \pm 0.4$ for water in the cortex + coat region (see the *SI Appendix*). The smaller DPF for this region is expected because the water content is higher than in the core. Because of fast water exchange between cortex and coat, we can only obtain the population-weighted average of the DPFs for these regions. We expect that ξ_{cx} is close to 1 because of the high water content in the cortex, whereas ξ_{ct} may be similar to ξ_{cr}.

The DPFs given in Table 2 should be regarded as upper bounds on the relative slowing down of water in the different spore compartments because the high-frequency ^{2}H relaxation rate may include a contribution from labile biopolymer deuterons in solvent-exposed OD and ND groups exchanging with D_2O deuterons on the millisecond time scale at pH 7.6 (34, 35). To assess the importance of labile deuterons, we measured the water-^{17}O relaxation rate at 81.3 MHz for the EDTA-treated sample. Because the relaxation time scale is much shorter for ^{17}O than for ^{2}H (22), the ^{17}O magnetization should also exchange slowly between the core and ncr regions. Nevertheless, the ^{17}O magnetization recovery appears to be monoexponential (Fig. S2*A* in the *SI Appendix*), presumably because fast transverse ^{17}O relaxation and/or dephasing due to local field inhomogeneities in the core causes the minor magnetization component to be lost during the 90-μs acquisition delay. The observed ^{17}O R_1 rate, which thus pertains to the ncr region, yields a DPF of $\xi_{ncr} = 2.69 \pm 0.02$ and, after correction for the ex fraction (as for the ^{2}H data), $\xi_{cx+ct} = 3.6 \pm 0.3$. This value is 25% smaller than the ^{2}H-derived DPF (Table 2). In contrast, for *Escherichia coli* cells at the same temperature and pH as here, the ^{2}H and ^{17}O DPFs do not differ significantly (23).

For the core, only the ^{2}H-derived DPF is available (Table 2). The labile-deuteron contribution in the core is probably negligibly small because the core pH is about one unit lower than in the ncr region (36) and because the DPF is much larger. Nevertheless, the ξ_{cr} value

in Table 2 should still be regarded as an upper bound because it may contain a small (outer-sphere) PRE contribution from the nonextractable Mn(II) ions in the core (see the *SI Appendix*).

Internal Water in Coat Proteins. We return now to the dominant low-frequency dispersion, focusing on the profile from EDTA-treated spores (Fig. 2, blue symbols). Similarly large low-frequency ^{2}H dispersions are obtained from immobilized globular proteins in cross-linked protein gels (24) or in bacterial cells (23) but not from freely tumbling proteins (22). This dispersion has been quantitatively linked to the escape of buried water molecules from small polar cavities inside the protein, rate-limited by intermittent protein conformational dynamics on the $10^{-8} - 10^{-5}$ s time scale (24).

As shown above, the MRD profile from WT spores reports on water dynamics in the ncr region outside the core. Because the cortex peptidoglycan network (18) is not expected to trap water molecules for periods >10 ns (35), the low-frequency dispersion must be produced by internal water molecule in the coat layers, comprising ≈55% of total spore protein (37). The coat proteins, organized in dense, cross-linked layers (20, 27), are expected to be rotationally immobilized and they should therefore contribute to the low-frequency dispersion (23, 24).

We determine the internal water fraction, f_{int}, by numerical integration of the dispersion profile (Fig. 2, blue area). Because this integral is rigorously independent of the unknown internal-water residence time distribution, it yields f_{int} in an essentially model-independent way (23, 38). With an upper integration limit of 1 MHz, f_{int} represents internal water molecules with residence times longer than 160 ns and shorter than ≈10 μs (23). In this way, we obtain $f_{int} = (1.0 \pm 0.1)\times10^{-3}$. We can then estimate the average prevalence of internal water in coat proteins, expressed as the number, ν_{int}, of internal water molecules per 100 aa residues (see the *SI Appendix*). The result, $\nu_{int} = 2.5 \pm 0.6$, is similar to the value 3.6 ± 1.0 derived in the same way for immobilized *E. coli* proteins and to the value 3.4 obtained from analysis of 842 protein crystal structures (39). The slightly lower value obtained here may reflect a lower internal-water content of coat proteins or a larger fraction of internal water molecules with residence times >10 μs (making them unobservable) in the extensively cross-linked (and hence less flexible) coat proteins. In any case, our analysis shows that the large low-frequency ^{2}H dispersion can be accounted for by a tiny fraction (0.14%) of spore water trapped inside proteins and that it does not indicate a drastic slowing down of a significant water population elsewhere in the spore.

Water Exchange Across the Inner Membrane. The finding that water exchange between the core and ncr regions is slow on the ^{2}H relaxation time scale provides an upper bound on the water permeability of the IM. Quantitatively, the observation of biexponential ^{2}H relaxation implies that the mean residence time of a water molecule in the core obeys the inequality (31) $\tau_{cr} > [(1 - f_{cr})(R_1^{cr} - R_1^{ncr})]^{-1}$. Inserting values from Table 1, we obtain $\tau_{cr} > 20$ ms. This result can be converted into an upper bound on the passive (diffusive) water permeability of the IM through the relation $P_w = \phi_w^{cr} a_{cr}/(3\tau_{cr})$, with the effective radius $a_{cr} = 3V_{cr}/A_{cr}$ determined by the volume and surface area of the core. Taking the dimensions of the assumed prolate-ellipsoidal core from Fig. 1, we find $a_{cr} = 0.20$ μm. By using $\phi_w^{cr} = 0.55 \pm 0.1$ for the volume fraction of water in the core (14, 17, 32), we thus obtain $P_w < 1.8 \pm 0.6$ μm s^{-1}.

We also recorded the water-^{2}H MRD profile (Fig. 2, red symbols) from spores of a *cotE gerE B. subtilis* strain lacking most of the proteinaceous coat (27). The fraction of missing coat protein, 87 ± 16%, was estimated from protein analysis of the WT and mutant spore preparations (see the *SI Appendix*). The mutant spores were also treated with EDTA, which removed the PRE peak at 6 MHz. For WT spores, the MRD profile reports on water dynamics outside the core. Because most of the protein in this region is concentrated in the coat, we expected the MRD profile for the mutant spores to fall well below that of the WT spores. [The R_1 data in Fig. 2 have been normalized to the same water mass fraction to compensate for the slightly different total water content in the samples (22).] But the ^{2}H relaxation rate for the mutant spores is higher at all frequencies. This paradox is resolved by examining the magnetization recovery at high frequencies.

In contrast to WT spores, mutant spores yield monoexponential ^{2}H relaxation at 92 MHz (Fig. S2*B* in the *SI Appendix*), implying fast water exchange across the IM (core water residence time <20 ms). R_1 thus reports on water dynamics in the entire spore, including the core region. If water exchange had been fast in the WT spore, we would have observed monoexponential ^{2}H relaxation at 92 MHz with $R_1 = f_{cr} R_1^{cr} + (1 - f_{cr}) R_1^{ncr} = 14.5^{-1}$, not far from the value measured for the mutant spores (Table 1). (Full agreement is not expected because of the loss of coat protein, which should decrease R_1^{ncr} and increase f_{cr}.)

The fast-exchange condition established at 92 MHz does not necessarily apply at low frequencies, where the much larger relaxation rate makes the condition more restrictive. Although the biexponential magnetization recovery expected under slow-exchange conditions would not have been observed with the field-cycling instrument (see the *SI Appendix*), the low-frequency dispersion is far too large to be produced by internal water molecules in the proteins of the severely decimated coat of the mutant spore. Indeed, a quantitative analysis shows that water exchange across the IM must be fast compared with the ^{2}H relaxation rate also at low frequencies (see the *SI Appendix*). We can then infer a more stringent upper bound on the mean residence time of a water molecule in the core: $\tau_{cr} < 0.8$ ms (see the *SI Appendix*). Converting the residence time into IM water permeability as before, we find $P_w > 46 \pm 14$ μm s^{-1}.

Discussion

Barriers to Water Transport Within the Spore. As compared to vegetative cells, spores are highly resistant to a wide range of toxic chemicals (2). The spore's first line of defense is the coat, the multiple protein layers of which act as a chemical filter. In addition, the core is physically protected by the low permeability of the IM. Whereas single-component phospholipid bilayers typically have water permeabilities in the range 50–300 μm s^{-1} (at 25° C) (40, 41), we find that $P_w < 1.8 \pm 0.6$ μm s^{-1} (at 27° C) for the IM of *B. subtilis* spores. The low water permeability of the IM is consistent with the slow uptake of methylamine by the core of *B. megaterium* spores (42). From the reported time, 2.5 h, for half maximal uptake (at 24° C) (42), we estimate a permeability for (deprotonated) methylamine of 0.1 μm s^{-1}. Because methylamine is less polar than water, this result suggests that the water permeability of the IM may be 1–2 orders of magnitude below our upper bound and thus 3–4 orders of magnitude lower than in simple bilayer membranes (40, 41).

According to the solubility-diffusion model of permeation, P_w is proportional to the product of diffusion coefficient, D_w, and partition coefficient of water in the membrane (43). The extremely low P_w thus indicates a drastic reduction of either or both of these factors in the IM. Diffusion measurements employing fluorescent labels have shown that 70% of the IM lipids in *B. subtilis* spores are immobile on a time scale of seconds, whereas the diffusion coefficient, D_{lipid}, of the remaining 30% is reduced by an order of magnitude compared with vegetative cells (21). The drastically reduced fluidity of the IM implied by these results is qualitatively consistent with the low water permeability inferred here because both D_w and D_{lipid} should be inversely proportional to the effective viscosity of the membrane. Furthermore, the relatively high core-water mobility found here indicates that the low lipid mobility is caused by membrane compression (and perhaps gel-state ordering) rather than by headgroup interactions with a glassy core interior.

The much larger water permeability $P_w > 46 \pm 14$ μm s^{-1}, found here for the IM of the coat-deficient mutant spores, is unexpected

and can only be explained by invoking major structural changes in the membrane. Presumably, the IM of mutant spores is also more permeable to other small molecules. Although the sensitivity of *cotE gerE* spores to hypochlorite has been linked to the loss of coat proteins (27), the enhanced permeability of the IM may also contribute to the impaired chemical resistance.

The spore coat, including the outer membrane, is not considered to be a significant permeability barrier for small molecules (2). Consistent with this view, our data indicate fast water exchange across the coat on the ^{2}H and ^{17}O relaxation time scales. Scanning microscope observation of *B. thuringiensis* spores exposed to variable humidity identified two distinct time scales, 50 and 500 s, for spore swelling, tentatively identified with water influx into the coat + cortex and into the core, respectively (44). These time scales refer to swelling of dried spores and they are much longer than the time scales found here for water exchange within fully hydrated spores. The longer time scale (500 s) corresponds to a water permeability of the IM of order 10^{-4} μm s^{-1}, 3 orders of magnitude less than for methylamine (see above). The shorter time scale (50 s) is 4 orders of magnitude longer than the upper bound for the water exchange time across the coat implied by the present NMR data.

The Core Is Not in a Glassy State. To compare the core-water DPF, $\xi_{cr} = 30.8 \pm 0.5$, with DPFs for water in other biological systems, we must take into account differences in water content. For this comparison, we quote hydration levels in units of g H_2O (g dry protein)$^{-1}$, conventionally denoted by h. For the core of the WT spores, we estimate a hydration level of 0.6 ± 0.1 h (see the *SI Appendix*). Monolayer coverage of a 20 kDa protein corresponds to 0.7 h (23). Because some of the core water hydrates nonprotein components, we conclude that the core proteins are surrounded by at most one water layer. With the possible exception of Ca^{2+} ions (see the *SI Appendix*), nonprotein components are not expected to contribute significantly to the core-water DPF (23).

The core-water DPF is twice as large as the DPF of 15.6 ± 3 for water in the macromolecular hydration layers of an *E. coli* cell (23), and it differs even more from the DPFs of 5–10 obtained for the hydration layer of proteins in dilute aqueous solution (45). These DPF differences can be understood by realizing that the DPF is an average over a wide distribution of hydration sites, with water correlation times ranging from a few ps to 2 ns. Hydration sites with correlation times approaching the upper limit of this range contribute disproportionately to the DPF (33). The defining feature of such strongly perturbing hydration sites is geometrical confinement, which prohibits collective rearrangement of the hydrogen-bond network in liquid water (33). On an "isolated" protein surface, these secluded hydration sites, usually deep pockets, are few in number, but additional secluded hydration sites are created when a (partial) hydration layer is confined between two protein surfaces. The increasing DPF trend in going from protein solution (10–100 h) to bacterial cell (3.2 h) to spore core (0.6 h) can thus be explained by the increasing prevalence of confined hydration layers as the water content decreases. This notion is consistent with water ^{2}H relaxation data from protein crystals and rehydrated protein powders. For protein crystals, DPF values range from 9 for tetragonal hen lysozyme at 0.52 h (46) to 40 for crambin at 0.34 h (47), whereas a DPF of 46 was reported for amorphous hen lysozyme powder hydrated to 0.25 h (48). In conclusion, the core-water DPF is consistent with DPF values from binary protein-water systems at comparable hydration levels. As for other systems, the majority of core water molecules are likely to be considerably more mobile than indicated by the DPF, which is dominated by a minority of water molecules in confined hydration sites. Furthermore, a significant contribution to the core-water DPF could come from relatively slow (but <2 ns) symmetric flip motions of water molecules coordinated to Ca^{2+} ions in the core (49).

If the core were in a glassy state, as conjectured (7–9), then core water would be in the "rigid lattice" NMR regime (correlation time $\gg 10^{-6}$ s), producing a $\approx$200 kHz wide ^{2}H NMR spectrum that would not contribute to the ^{2}H NMR signal detected here. However, we find that, on average, core water is "only" 30-fold less mobile than bulk water. Because the rotational correlation time for bulk H_2O is 1.6 ps at 27° C, $\xi_{cr} = 30.8$ corresponds to a mean rotational correlation time of $30.8 \times 1.6 \approx 50$ ps for core water. We therefore conclude that the core is not in a glassy state. Fully hydrated proteins undergo a broad intramolecular dynamical transition to a glass-like state but only at low temperatures (180–220 K) (50). A similar transition is observed near room temperature for protein powders (50) but only at water contents ($\approx$0.1 h) much lower than in the core ($\approx$0.6 h). Our results on core-water mobility are therefore consistent with the behavior of simpler systems.

Water behavior in biological systems is often described in terms of "free" and "bound" water, with the tacit assumption that bound water is largely immobile. These terms lack precision and are often misleading. If a water molecule is extensively hydrogen-bonded, whether to proteins or to adjacent water molecules, it strongly prefers this environment to a noninteracting state (water vapor). However, hydrogen bonds per se do not immobilize a water molecule, as seen by considering bulk water. Core water is both bound and mobile, and there is no contradiction in this.

Origin of Dormancy and Heat Resistance. In binary protein–water systems, protein tumbling is effectively quenched at hydration levels $<$1.5 h (51). In the core (at 0.6 h), proteins are thus not expected to undergo translational or rotational diffusion at measureable rates. This expectation is consistent with fluorescence studies (14) and with our analysis of the low-frequency ^{2}H dispersion (Fig. 2) in terms of internal water molecules in rotationally immobilized proteins. However, protein immobilization does not preclude enzyme activity as long as substrates can diffuse within the core. As noted above, most core water is expected to be much more mobile than indicated by the DPF. The rate of substrate diffusion in the core of the dormant spore may therefore be of the same order of magnitude as in the vegetative cell. Unlike eukaryotic organisms that achieve dormancy by replacing water with glass-forming disaccharides (5, 6), bacterial spores can apparently inhibit metabolism without immobilizing the solvent. This conclusion may seem surprising because purified enzymes may show significant activity at hydration levels as low as 0.2 h (50). However, water is probably not evenly distributed within the core. Key enzymes may therefore be sufficiently dehydrated that they cannot access conformations required for activity (52).

Heat inactivation of spores typically requires temperatures 40° C above what is needed to kill the corresponding vegetative cells (1, 2). Moreover, for *Bacillus* spores, heat resistance decreases exponentially with increasing core water content in the range 28–57% (17). Core dehydration might improve heat resistance by stabilizing proteins against thermal denaturation (50, 53), presumably by disfavoring the unfolded state entropically (by excluding extended polypeptide conformations) as well as energetically (by restricting availability of water molecules for replacing intraprotein hydrogen bonds). However, to raise the heat denaturation temperature by 40° C in binary systems requires dehydration to $\approx$0.1 h, whereas little or no stabilization is seen at the hydration level (0.6 h) of the spore core (50, 53).

If core dehydration does not confer heat resistance directly by stabilizing proteins against thermal denaturation, it might act indirectly by immobilizing proteins, thereby preventing irreversible protein aggregation. As long as heat denaturation is reversible, it should not kill the spore. Indeed, protein lyophilization may induce (partial) unfolding (54), but this is usually a reversible process. Only at hydration levels high enough to permit intermolecular disulfide

exchange or entanglement does unfolding lead to irreversible protein aggregation (55), which would compromise the viability of the spore. This view is also consistent with Raman spectra of single *B. subtilis* spores, indicating that heat activation at a sublethal temperature of 70° C is accompanied by partial but reversible protein denaturation (56).

Materials and Methods

***B. subtilis* Strains.** The two *B. subtilis* strains used here are isogenic derivatives of strain PS832, a prototrophic laboratory derivative of strain 168. The WT strain PS533 (57) carries a plasmid pUB110 encoding resistance to kanamycin, and the coat-deficient strain PS4150 (27) is deleted for most of the *cotE* and *gerE* coding sequences. The CotE protein is essential for assembly of many coat proteins and of the outer layer and GerE is a DNA-binding protein that, in addition to other activities, regulates transcription of several coat protein genes (19, 20). In the text, spores from the strains PS533 and PS4150 are referred to as WT and mutant spores, respectively.

Spore Preparation. Spores were prepared at 37° C on 2×SG medium agar plates, and were harvested, cleaned and stored as described (58, 59). All spore preparations used were free (> 99%) from growing or sporulating cells, germinated spores and cell debris as determined by phase contrast microscopy.

Preparation of NMR Samples. The spores were dissolved in 5 mM phosphate/D_2O buffer at pH 7.6. After centrifugation at 6,800 × *g*, the spore mass was transferred to an NMR tube insert. Manganese depleted samples were first suspended in 10 mM EDTA and washed twice. After completion of NMR measurements, the samples were dried to determine the water content and they were then subjected to elemental analysis (Table S1 of the *SI Appendix*) and complete amino acid analysis (Table S3 of the *SI Appendix*). For further details, see the *SI Appendix*.

NMR Experiments. The longitudinal relaxation rate R_1 of the water-^{2}H magnetization was measured from 1.5 kHz to 92.1 MHz by using six different NMR instruments, and the water-^{17}O R_1 was measured at 81.3 MHz. All NMR experiments were performed within 3 days at a temperature of 27 ± 0.1° C. Biexponential magnetization curves were fitted with the function $M_z(t) - M_z(\infty) = [M_z\,(0) - M_z(\infty)]\,[f_{cr}\exp(-R_1^{cr}t) + (1 - f_{cr})\exp(-R_1^{ncr}t)]$. For further details, see the *SI Appendix*.

ACKNOWLEDGMENTS. This work was supported by grants from the Swedish Research Council (to B.H. and L.H.), the Knut and Alice Wallenberg Foundation (to B.H.), and the US Army Research Office (to P.S.).

1. Gerhardt P, Marquis RE (1989) Spore thermoresistance mechanisms. In *Regulation of Procaryotic Development*, eds Smith I, Slepecky RA, Setlow P (Am Soc Microbiol, Washington, DC), pp 43–63.
2. Setlow P (2006) Spores of *Bacillus subtilis*: Their resistance to and killing by radiation, heat and chemicals. *J Appl Microbiol* 101:514–525.
3. Nicholson WL, Munakata N, Horneck G, Melosh HJ, Setlow P (2000) Resistance of *Bacillus* endopsores to extreme terrestrial and extraterrestrial environments. *Microbiol Mol Biol Rev* 64:548–572.
4. Dill KA (1990) Dominant forces in protein folding. *Biochemistry* 29:7133–7155.
5. Crowe JH, Carpenter JF, Crowe LM (1998) The role of vitrification in anhydrobiosis. *Annu Rev Physiol* 60:73–103.
6. Buitink J, Leprince O (2008) Intracellular glasses and seed survival in the dry state. *Comptes Rendus Biologies* 331:788–795.
7. Gould GW (1986) Water and the survival of bacterial spores. In *Membranes, Metabolism, and Dry Organisms*, ed Leopold AC (Cornell Univ Press, Ithaca), pp 143–156.
8. Sapru V, Labuza TP (1993) Glassy state in bacterial spores predicted by polymer glass-transition theory. *J Food Sci* 58:445–448.
9. Ablett S, Darke AH, Lillford PJ, Martin DR (1999) Glass formation and dormancy in bacterial spores. *Int J Food Sci Technol* 34:59–69.
10. Leuschner RGK, Lillford PJ (2003) Thermal properties of bacterial spores and biopolymers. *Int J Food Microbiol* 80:131–143.
11. Carstensen EL, Marquis RE, Child SZ, Bender GR (1979) Dielectric properties of native and decoated spores of *Bacillus megaterium*. *J Bacteriol* 140:917–928.
12. Johnstone K, Stewart GSAB, Barratt MD, Ellar DJ (1982) An electron paramagnetic resonance study of the manganese environment within dormant spores of *Bacillus megaterium* KM. *Biochim Biophys Acta* 714:379–381.
13. Leuschner RGK, Lillford PJ (2000) Effects of hydration on molecular mobility in phase-bright *Bacillus subtilis* spores. *Microbiology* 146:49–55.
14. Cowan AE, Koppel DE, Setlow B, Setlow P (2003) A soluble protein is immobile in dormant spores of *Bacillus subtilis* but is mobile in germinated spores: Implications for spore dormancy. *Proc Natl Acad Sci USA* 100:4209–4214.
15. Maeda Y, Fujita T, Sugiura Y, Koga S (1968) Physical properties of water in spores of *Bacillus megaterium*. *J Gen Appl Microbiol* 14:217–226.
16. Bradbury JH, Foster JR, Hammer B, Lindsay J, Murrell WG (1981) The source of the heat resistance of bacterial spores. Study of water in spores by NMR. *Biochim Biophys Acta* 678:157–164.
17. Beaman TC, Gerhardt P (1986) Heat resistance of bacterial spores correlated with protoplast dehydration, mineralization, and thermal adaption. *Appl Environ Microbiol* 52:1242–1246.
18. Popham DL (2002) Specialized peptidoglycan of the bacterial endospore: The inner wall of the lockbox. *Cell Mol Life Sci* 59:426–433.
19. Driks A (1999) *Bacillus subtilis* spore coat. *Microbiol Mol Biol Rev* 63:1–20.
20. Henriques AO, Moran CP (2000) Structure and assembly of the bacterial endospore coat. *Methods* 20:95–100.
21. Cowan AE, et al. (2004) Lipids in the inner membrane of dormant spores of *Bacillus* species are largely immobile. *Proc Natl Acad Sci USA* 101:7733–7738.
22. Halle B, Denisov VP, Venu K (1999) Multinuclear relaxation dispersion studies of protein hydration. In *Biological Magnetic Resonance*, eds Krishna NR, Berliner LJ (Kluwer Academic, New York), Vol 17, pp 419–484.
23. Persson E, Halle B (2008) Cell water dynamics on multiple time scales. *Proc Natl Acad Sci USA* 105:6266–6271.
24. Persson E, Halle B (2008) Nanosecond to microsecond protein dynamics probed by magnetic relaxation dispersion of buried water molecules. *J Am Chem Soc* 130:1774–1787.
25. Abragam A (1961) *The Principles of Nuclear Magnetism* (Clarendon Press, Oxford).
26. Marshall BJ, Murrell WG (1970) Biophysical analysis of the spore. *J Appl Bact* 33:103–129.
27. Ghosh S, et al. (2008) Characterization of spores of *Bacillus subtilis* that lack most coat layers. *J Bacteriol* 190:6741–6748.
28. Koenig SH, Brown RD (1985) Relaxation of solvent protons and deuterons by protein-bound Mn^{2+} ions. Theory and experiment for Mn^{2+}-concanavalin A. *J Magn Reson* 61:426–439.
29. Bertini I, Luchinat I, Parigi G (2005) ^{1}H NMRD profiles of paramagnetic complexes and metalloproteins. *Adv Inorg Chem* 57:105–172.
30. Kowalewski J, Kruk D, Parigi G (2005) NMR relaxation in solution of paramagnetic complexes: Recent theoretical progress for $S \geq 1$. *Adv Inorg Chem* 57:41–104.
31. Zimmerman JR, Brittin WE (1957) Nuclear magnetic resonance studies in multiple phase systems: Lifetime of a water molecule in an adsorbing phase on silica gel. *J Phys Chem* 61:1328–1333.
32. Nakashio S, Gerhardt P (1985) Protoplast dehydration correlated with heat resistance of bacterial spores. *J Bacteriol* 162:571–578.
33. Mattea C, Qvist J, Halle B (2008) Dynamics at the protein-water interface from ^{17}O spin relaxation in deeply supercooled solutions. *Biophys J* 95:2951–2963.
34. Denisov VP, Halle B (1995) Hydrogen exchange and protein hydration: The deuteron spin relaxation dispersions of bovine pancreatic trypsin inhibitor and ubiquitin. *J Mol Biol* 245:698–709.
35. Vaca Chávez F, Hellstrand E, Halle B (2006) Hydrogen exchange and hydration dynamics in gelatin gels. *J Phys Chem B* 110:21551–21559.
36. Setlow B, Setlow P (1980) Measurements of the pH within dormant and germinated bacterial spores. *Proc Natl Acad Sci USA* 77:2474–2476.
37. Goldman RC, Tipper DJ (1978) Bacillus subtilis spore coats: Complexity and purification of a unique polypeptide component. *J Bacteriol* 135:1091–1106.
38. Halle B, Jóhannesson H, Venu K (1998) Model-free analysis of stretched relaxation dispersions. *J Magn Reson* 135:1–13.
39. Park S, Saven JG (2005) Statistical and molecular dynamics studies of buried waters in globular proteins. *Proteins* 60:450–463.
40. Huster D, Jin AJ, Arnold K, Gawrisch K (1997) Water permeability of polyunsaturated lipid membranes measured by ^{17}O NMR., *Biophys J* 73:855–864.
41. Mathai JC, Tristram–Nagle S, Nagle JF, Zeidel ML (2008) Structural determinants of water permeability through the lipid membrane. *J Gen Physiol* 131:69–76.
42. Swerdlow BM, Setlow B, Setlow P (1981) Levels of H^+ and other monovalent cations in dormant and germinating spores of *Bacillus megaterium*. *J Bacteriol* 148:20–29.
43. Finkelstein A (1987) *Water Movement Through Lipid Bilayers, Pores, and Plasma Membranes.* (Wiley, New York).
44. Westphal AJ, Price PB, Leighton TJ, Wheeler KE (2003) Kinetics of size changes of individual *Bacillus thuringiensis* spores in response to changes in relative humidity. *Proc Natl Acad Sci USA* 100:3461–3466.
45. Halle B (2004) Protein hydration dynamics in solution: a critical survey. *Philos Trans R Soc London Ser B* 359:1207–1224.
46. Usha MG, Speyer J, Wittebort RJ (1991) Dynamics of the hydrate and amide groups of crystalline ribonuclease and lysozyme. *Chem Phys* 158:487–500.
47. Usha MG, Wittebort RJ (1989) Orientational ordering and dynamics of the hydrate and exchangeable hydrogen atoms in crystalline crambin. *J Mol Biol* 208:669–678.
48. Peemoeller H, Yeomans FG, Kydon DW, Sharp AR (1986) Water molecule dynamics in hydrated lysozyme. A deuteron magnetic resonance study. *Biophys J* 49:943–948.
49. Denisov VP, Halle B (1995) Direct observation of calcium-coordinated water in calbindin D_{9k} by nuclear magnetic relaxation dispersion. *Biochemistry* 117:8456–8465.
50. Gregory RB (1995) Protein hydration and glass transition behavior. In *Protein-Solvent Interactions*, ed Gregory RB (M Dekker, New York), pp 191–264.
51. Kimmich R, Gneiting T, Kotitschke K, Schnur G (1990) Fluctuations, exchange processes, and water diffusion in aqueous protein systems. A study of bovine serum albumin by diverse NMR techniques. *Biophys J* 58:1183–1197.
52. Setlow P (1994) Mechanisms which contribute to the long-term survival of spores of *Bacillus* species. *J Appl Bact* 76:49S–60S.
53. Rupley JA, Careri G (1991) Protein hydration and function. *Adv Prot Chem* 41:37–172.
54. Desai UR, Osterhout JJ, Klibanov AM (1994) Protein structure in the lyophilized state: A hydrogen isotope exchange / NMR study with bovine pancreatic trypsin inhibitor. *J Am Chem Soc* 116:9420–9422.
55. Klibanov AM, Schefiliti JA (2004) On the relationship between conformation and stability in solid pharmaceutical protein formulations. *Biotechnol Lett* 26:1103–1106.
56. Zhang P, Setlow P, Li Y (2009) Characterization of single heat-activated *Bacillus* spores using laser tweezers Raman spectroscopy. *Optics Express* 17:16480–16491.
57. Setlow B, Setlow P (1996) Role of DNA repair in *Bacillus subtilis* spore resistance. *J Bacteriol* 178:3486–3495.
58. Nicholson WL, Setlow P (1990) Sporulation, germination and outgrowth. In *Biological Methods for Bacillus*, eds Harwood CR, Cutting SM (Wiley, Chichester, UK), pp 391–450.
59. Paidhungat M, Setlow B, Driks A, Setlow P (2000) Characterization of spores of *Bacillus subtilis* which lack dipicolinic acid. *J Bacteriol* 182:5505–5512.
60. Erlendsson LS, Möller M, Hederstedt L (2004) Bacillus subtilis StoA is a thiol-disulfide oxidoreductase important for spore cortex synthesis. *J Bacteriol* 186:6230–6238.